Published in final edited form as:
Cancer Gene Ther. 2014 November ; 21(11): 472–482. doi:10.1038/cgt.2014.53.

Bortezomib sensitizes non-small cell lung cancer to mesenchymal stromal cell-delivered inducible caspase-9-mediated cytotoxicity

Miki Ando[#1,3], **Valentina Hoyos**[#1], **Shigeki Yagyu**[1], **Wade Tao**[1], **Carlos A. Ramos**[1], **Gianpietro Dotti**[1], **Malcolm K. Brenner**[1], and **Lisa Bouchier-Hayes**[1,2,‡]

[1]Center for Cell and Gene Therapy, Baylor College of Medicine, Texas Children's Hospital, and Houston Methodist Hospital, Houston, Texas, USA

[2]Department of Pediatrics-Hematology, Baylor College of Medicine, Houston, Texas, USA

[#] These authors contributed equally to this work.

Abstract

Delivery of suicide genes to solid tumors represents a promising tumor therapy strategy. However, slow or limited killing by suicide genes and ineffective targeting of the tumor has reduced effectiveness. We have adapted a suicide system based on an inducible caspase-9 (iC9) protein that is activated using a specific chemical inducer of dimerization (CID) for adenoviral based delivery to lung tumors via mesenchymal stromal cells (MSC). Four independent human non-small cell lung cancer (NSCLC) cell lines were transduced with adenovirus encoding iC9 and all underwent apoptosis when iC9 was activated by adding CID. However, there was a large variation in the percentage of cell killing induced by CID across the different lines. The least responsive cell lines were sensitized to apoptosis by combined inhibition of the proteasome using bortezomib. These results were extended to an *in vivo* model using human NSCLC xenografts. E1A-expressing MSC replicated Ad.iC9 and delivered the virus to lung tumors in SCID mice. Treatment with CID resulted in some reduction of tumor growth but addition of bortezomib led to greater reduction of tumor size. The enhanced apoptosis and anti-tumor effect of combining MSC-delivered Ad.iC9, CID and bortezomib appears to be due to increased stabilization of active caspase-3, since proteasomal inhibition increased the levels of cleaved caspase-9 and caspase-3. Knockdown of XIAP, a caspase inhibitor that targets active caspase-3 to the proteasome, also sensitized iC9-transduced cells to CID, suggesting that blocking the proteasome counteracts XIAP to permit apoptosis. Thus, MSC-based delivery of the iC9 suicide gene to human NSCLC effectively targets lung cancer cells for elimination. Combining this therapy with bortezomib, a drug that is otherwise inactive in this disease, further enhances the anti-tumor activity of this strategy.

[‡]To whom correspondence should be addressed: lxbouchi@txch.org.
[3]Current Address: Division of Stem Cell Therapy, Center for Stem Cell Biology and Regenerative Medicine, The Institute of Medical Science, The University of Tokyo, Minato-ku, Tokyo, Japan

INTRODUCTION

One suggested means by which solid tumors may be debulked is by introducing suicide genes that can be triggered by small molecule drugs.[1] Since these suicide systems can be designed to be non-cross resistant with conventional agents, they could potentiate available therapeutic regimens without a concomitant increase in toxicity. Despite initial promise however, many of these earlier suicide systems proved to be less clinically effective than desired, in part because of slow and limited killing of non-dividing or slowly dividing tumor compartments and in part because of limitations in methods used to deliver the suicide gene to the tumor.[1, 2]

We have previously reported the use of an inducible version of caspase-9 (iC9) as a suicide gene to increase the safety of adoptive cell therapies.[3-5] iC9 consists of the pro-apoptotic protein caspase-9, fused to a modified human FK-binding protein that can be conditionally dimerized following exposure to a chemical inducer of dimerization (CID), such as AP1903, or its functionally identical analog AP20187. Caspase-9 is thus activated by dimerization[6] resulting in apoptosis. In a clinical study, infused iC9–expressing donor T cells underwent rapid apoptosis when exposed to a single dose of the otherwise bioinert small molecule, AP1903, dramatically resolving symptoms due to graft versus host disease (GVHD).[3] Similarly, in a murine model, infused mesenchymal stromal cells (MSC) expressing iC9 were selectively eliminated following exposure to CID.[4] This strategy is highly effective as a safety-switch to limit potentially harmful side-effects of transferred cells, but the feasibility of using caspase-9 as a direct tumor killing mechanism is untested.

Caspase-9 is activated downstream of the mitochondrial pathway in response to diverse pro-apoptotic stimuli.[7] Direct dimerization of caspase-9 therefore bypasses many upstream signals, such as Bcl-2 overexpression, that may be present in tumor cells and are known to confer resistance to apoptosis.[8] This allows for direct and specific induction of apoptosis. Nonetheless, despite these putative benefits, downstream signals remain that may block or impede caspase-9-induced cell death. This could lead to significant heterogeneity in sensitivity to apoptosis induced by iC9 between distinct tumors, and between individual tumor cells within the same tumor. Inhibition of the proteasome with agents such as bortezomib has been shown to sensitize cells to apoptosis induced by a number of different stimuli, and produces these benefits in part by enhancing caspase activation.[9-12] We therefore also determined if the combination of iC9 and the protesomal inhibitor bortezomib can synergize and increase the killing of lung tumor cells. Although bortezomib is approved for the treatment of multiple myeloma and mantle cell lymphoma, it has little clinical efficacy against lung cancer and other solid tumors as a single agent.[13]

Due to the known difficulties in effectively delivering suicide genes to patients with lung cancer, we determined if we could use MSC to deliver iC9 to non-small cell lung cancer in vivo. MSC have already been used to deliver a number of different genes to tumors including tumor necrosis factor apoptosis-inducing ligand (TRAIL), interleukin-12 and interferon.[14-17] Here we determine if MSC can also be adapted to transfer iC9.

To enhance transfer of the iC9 to tumor cells, we modified the MSC to produce an adenovirus encoding iC9. Adenoviruses can infect quiescent cells and hence can effectively deliver suicide genes to tumors, but systemic administration of high doses of virus is associated with systemic toxicity[18] and rapid elimination of the virus by the immune system before reaching the tumor.[19] Toxicity is limited and viral delivery is enhanced when MSC are used as vehicles.[20] This strategy may be particularly effective for the delivery of suicide genes to lung tumors since MSC have been shown to accumulate in the lung vascular bed after intravenous administration[21] and to selectively migrate to sites of malignancy.[22-24] We therefore prepared a replication incompetent (E1A deleted) adenoviral vector containing *iC9*. Additional forced expression of E1A in the MSC converted human MSC into Adenoviral-iC9 (Ad-iC9) producer cells. We now report how MSC-mediated delivery of Ad.iC9 can be combined with bortezomib to produce significant anti-tumor activity in a human xenograft model, even in otherwise resistant tumors.

MATERIALS AND METHODS

Reagents

CID/AP20187 was purchased from Clontech as B/B homodimerizer and diluted in 100% Ethanol. The proteasome inhibitor bortezomib and pan-caspase inhibitor qVD-Oph were purchased from Selleck Chemicals and R&D Systems, Inc., respectively and dissolved in DMSO.

Cloning

The construction of the iC9 suicide cassette was previously described.[25] Briefly, the caspase recruitment domain (CARD) of the caspase-9 gene was replaced with a 12-kDa human FK506 binding domain (FKBP12; GenBank AH002 818). Caspase-9 was fused via a 2A-derived nucleotide sequence to truncated human CD19 (iC9-ΔCD19). As previously demonstrated, fusion of FKBP to caspase-9 enables conditional dimerization and activation of the caspase by addition of a Chemical Inducer of Dimerization (CID/AP20187), a ligand containing two FK506 moieties, to the cellular medium.[5] Recombinant Adenovirus 5F35 was constructed using the Adeno-X™ Expression System 1 from Clontech. The iC9-ΔCD19 sequence was amplified by PCR and inserted into the pShuttle 2 plasmid. The recombinant expression cassette was then digested using I-*Ceu* I and PI-*Sce* I and subcloned into the Adeno-X™ genome. The vector encoding the fusion protein eGFP-Fireflyluciferase (eGFP-FFLuc) was previously described[26]. The retrovirus vector encoding Adenovirus E1A 12s gene was obtained from Addgene (pWZL-E1A-Hygro, #18750).

Virus production

The retroviral supernatant was prepared by transfecting 293T cells with the retroviral construct, Peg-Pam-e encoding for *gag-pol*, and RDF encoding for the RD114 envelop using Fugene6 transfection reagent (Roche, Indianapolis, IN), and supernatants were collected 48 and 72 hours later. Adenovirus was produced by Baylor College of Medicine (BCM) Vector Development lab following standard operating procedures (www.bcm.edu/vector)

Generation of MSC

MSC were isolated from healthy donors (following a standard BCM Institutional Review Board approved protocol) as described previously.[4] Discarded (post infusion) healthy donor bone marrow collection bags and filters were washed with RPMI 1640 and plated on tissue culture flasks in RPMI with 10% fetal bovine serum (FBS), 2 mM L-glutamine, 100 units/ml penicillin, and 100 mg/ml streptomycin (Invitrogen). After 48 hours, the supernatant was discarded and the cells were cultured in complete culture medium: α-MEM (Invitrogen) with 16.5% FBS, 2 mM alanyl-glutamine, 100 units/ml penicillin, and 100 mg/ml streptomycin. Cells were grown to less than 80% confluency and re-plated at a lower density. The bone marrow-derived MSC used in the present study exhibited a spindle shape, expressed MSC-defining markers measured by flow cytometry analysis, and differentiated into adipocytes, osteocytes, and chondrocytes in appropriate culture media (data not shown).

Cell Culture

Human non-small cell lung cancer cell lines (H1299, H441, H1650, and A549) were obtained from American Type Culture Collection. H1299, H441 and H1650 were cultured in RPMI 1640 and A549 were cultured in Dulbecco's modified Eagle's medium (DMEM). All media was supplemented with 10% fetal bovine serum and 2 mM L-glutamine. Cells were grown at 37°C in a humidified incubator at 5% CO_2.

Adenoviral Transduction

Cells were plated in a 6 well tissue culture treated plate (1×10^5 cells/well) and cultured in corresponding complete medium for 24 hr. Medium was aspirated and replaced with 250 μL serum free IMDM medium per well. Ad.iC9 at 1500 VP/cell was added and plates were rocked every 10 min for one hour and every 20 min for the following 2 hours. Next, 650 μL of corresponding complete medium was added per well. Cells were collected after 72 hr and stained with anti-CD19-APC antibody according to the manufacturer's instructions (BD Biosciences). The percentage of cells expressing ΔCD19 was measured by flow cytometry (Gallios, Beckman Coulter) 72 hr after transduction.

Xenograft mouse model

All mouse experiments followed BCM animal husbandry guidelines. Seven-week old severe combined immunodeficient female BEIGE mice (CB17-SCID; Charles River) were inoculated via tail vein injection with 2.5×10^6 A549 cells labeled with firefly luciferase (FFLuc). Tumor engraftment was measured using the Xenogen-IVIS Imaging System (Caliper Life Sciences, Hopkinton, MA, USA). Mice were injected intraperitoneally (i.p.) twice a week with D-luciferin (150mg/kg), and signal intensity was measured as total photon/sec/cm^2/sr (p/s/cm^2/sr). On day 4 after tumor establishment, Ad.iC9-transduced E1A-MSC (1×10^6) were infused into mice in the treatment groups via tail vein injection. 48 hours later, the corresponding groups were treated with CID (50 μg) i.p. 2 to 3 doses every other day and bortezomib (0.3 mg/kg) i.p. twice a week for one week. The treatment cycle was repeated once.

Measurement of Apoptosis

Cells were treated as indicated, trypsinized, and collected by centrifugation. Cells were stained with Annexin-V PE and 7-amino-actinomycin D (7-AAD) for 15 minutes according to manufacturer's instructions (BD Biosciences). Annexin V/7-AAD-positive cells were quantified by flow cytometry (Gallios, Beckman Coulter) and analyzed with Kaluza software (Beckman Coulter). To inhibit apoptosis, the pan-caspase inhibitor qVD-OPh (20 μM) was added 48 hours after Ad.iC9 transduction.

Antibodies and Immunoblot

Cells were treated as indicated, trypsinized, and collected by centrifugation. Cells were resuspended in RIPA buffer (Cell Signaling Technology) containing protease inhibitor and incubated for 30 minutes on ice. After 30 minutes centrifugation, supernatant was harvested, mixed 1:2 with Laemmli buffer (Bio-Rad) and boiled. Equivalent amounts of protein were resolved by 4-12% SDS-polyacrylamide gels. Proteins were transferred to PVDF membranes (Bio-Rad) and probed with polyclonal rabbit antibodies specific for caspase-9, cleaved caspase-9 and caspase-3 and with monoclonal rabbit antibodies specific for cleaved caspase-3 and XIAP (Cell Signaling Technology). Blots were exposed to goat anti-rabbit HRP conjugate secondary antibody and proteins were detected using enhanced chemiluminescence (ECL) substrate for horseradish peroxidase (HRP) enzyme kit (Thermo Scientific). The membranes were stripped and reprobed with HRP-conjugate mouse monoclonal anti-actin (Santa Cruz Biotechnology).

Lentivirus mediated knockdown of XIAP

GIPZ lentiviral based shRNA constructs that contain mir30 sequences and GFP targeting XIAP, GAPDH or non silencing random sequences were purchased from Open Biosystems. (Clone IDs: V2LXX_00001, V2LXX_00002, V2LHS_94574, V3LHS_302102 and V3LHS_302105). Lentivirus production and infection with lentiviral shRNA supernatant followed the manufacturer's instructions using TransLenti Viral GIPZ Packaging System (Thermo Scientific Open Biosystems Catalog #TLP4614, TLP4615). Cells were selected by culture with puromycin 1 μg/mL and then sorted for high GFP expression (top 10%).

Statistical analysis

All statistical analyses used GraphPad Prism 4.0 software (GraphPad Software). Paired two-tailed Student's t test was used to determine the statistical significance of differences between samples. All numerical data are represented as mean ± 1 standard deviation. Results were considered statistically significant when $p < 0.05$.

RESULTS

NSCLC tumor cells transduced with inducible caspase-9 (iC9) undergo apoptosis in the presence of Chemical Inducer of Dimerization (CID)

We cloned an inducible version of caspase-9 (iC9), consisting of the catalytic domains of caspase-9 fused to the FKBP dimerization domain, into the adenoviral vector Ad5F35 (**Fig. 1a**).[27] To assess the efficiency of apoptosis induced by iC9 activation in a lung tumor

model, we transduced a number of independently generated non-small cell lung cancer (NSCLC) cell lines, including H1299, A549, H441 and H1650, with adenoviral iC9 (Ad.iC9). Treatment of non-transduced cells with CID did not induce measurable apoptosis (**Supplemental Figure S1**) confirming that this compound is bioinert when used at these concentrations.[28] On day 3 after transduction, CID was added. Apoptosis was determined 24 hours later by Annexin V and 7-AAD staining, and quantified by flow cytometry. Expression of iC9 alone induced negligible amounts of apoptosis in H1299 and A549 cells, while slightly higher levels (up to 30%) were detected in H441 and H1650 cell lines. Addition of CID to H1299 cells and H441 cells induced robust apoptosis, confirming that enforced dimerization of caspase-9 induced programmed cell death (**Fig. 1b**). In contrast, addition of CID to the remaining two cell lines, A549 and H1650, produced substantially lower levels of apoptosis (**Fig. 1b**). Thus iC9 appears to induce apoptosis with variable efficiency across the NSCLC cell lines tested.

To determine if differences in sensitivity to apoptosis reflected differences in transduction efficiency, we measured expression of iC9 in a number of different ways. The iC9 sequence was linked to a truncated form of CD19 (ΔCD19) by the self-cleaving 2A sequence. This truncation mutant of CD19 has no activity, but is still recognized by antibodies allowing us to measure expression of the linked iC9 protein. Expression of ΔCD19, was measured by flow cytometry and showed that all cell lines were comparably transduced at greater than 80% efficiency (**Fig. 1c**, *upper panel*). The MFI (mean fluorescence index) indicated the total ΔCD19 expressed (**Fig. 1c,** *lower panel*). H1299, H441 and A549 showed similar levels of ΔCD19 expression, while H1650 showed lower levels of ΔCD19 expression in comparison. iC9 expression levels, as measured by Western blot, showed a very similar pattern of relative expression of iC9 with the levels being lowest in H1650 cells (**Fig. 1d**). Although there were differences in the relative levels of iC9 protein expression, these did not correlate with the differences in sensitivity to apoptosis that we observed. For example, A549 cells were much more resistant to iC9-induced apoptosis than H1299 cells despite similar amounts of iC9 protein expressed. Therefore, the variability in iC9-induced apoptosis across the NSCLC cell lines was not a result of differential iC9 expression.

iC9-induced apoptosis is enhanced by proteasome inhibition

The proteosome inhibitor bortezomib is used clinically and can overcome resistance to other cytotoxic drugs and sensitize cells to diverse apoptosis inducers.[13] To maximize apoptosis induced by iC9 in the NSCLC cell lines, we investigated the effect of co-treatment with bortezomib. Treatment of non-transduced cells and iC9-transduced cells with bortezomib alone did not induce apoptosis (**Fig. 2a**). In the iC9-transduced cell lines, H1299 and H441, in which CID induced the highest levels of apoptosis, the addition of bortezomib (80nM) had little further effect. However in H1650 and A549 cells, the combination of bortezomib and CID consistently enhanced apoptosis of iC9-transduced cells above the levels induced by iC9 activation alone (**Fig. 2a**). Of note, in H1299 cells, bortezomib induced apoptosis of iC9-transduced cells even in the absence of the dimerizing drug. This may indicate that inhibition of the proteasome leads to stabilization of spontaneous dimerization of FKBP-caspase-9 in the absence of CID in this cell line.

To determine if the combined effects of bortezomib and CID were synergistic or merely additive, we further characterized the cell line that appeared to be most sensitive to caspase-9-induced apoptosis, H1299, and the cell line that appeared to be most resistant, A549. We treated each iC9-transduced cell line with increasing concentrations of bortezomib alone, CID alone, or a combination of both drugs. iC9-transduced A549 cells showed a synergistic response to bortezomib and CID as determined by median drug effect analyses (**Fig. 2b, Supplemental Figure S2**). The combination index (CI) values for the A549 cell line were 0.002-0.003 for doses of 10-160 nM demonstrating synergism as defined by CI<1 (**Fig. 2c**). In contrast, H1299 cells only showed synergy (0.267, 0.808) at 40 nM and 80 nM doses of combined CID and bortezomib respectively, while the remaining doses (10 nM, 20 nM and 160 nM) showed slight antagonism (CI>1).

Delivery of iC9 to lung tumor cells by mesenchymal stromal cells (MSC).

We next investigated the feasibility of delivering Ad.iC9 to lung tumor cells. We used MSC as the vehicle, exploiting the propensity of these cells to be trapped in lung vasculature and to migrate towards tumor sites.[21, 24] Since Ad.iC9 is a replication incompetent vector, we first transduced MSC with a retroviral vector encoding the adenoviral gene E1A to allow active adenoviral replication. Five days following transduction, 20 to 60% of transduced MSC expressed E1A, as determined by immunofluorescence staining for E1A (**Fig. 3a**). To test if these cells produced infectious adenovirus, E1A-negative (E1A−) and E1A-positive (E1A+) MSC were infected with a GFP-encoding adenoviral vector (Ad.GFP). We infected each MSC population with Ad.GFP at 1500 VP/cell, removed the supernatant after 5 days and then added the supernatant to H1299 cells to compare the titers of infectious AdV produced by each. As shown in **Fig. 3b**, after 48 hours, 93.4±4.6% of H1299 cells exposed to supernatant from E1A+ MSC became GFP positive, versus 29.1±14.4% of H1299 cells exposed to supernatant from E1A− MSC ($p = 0.0018$). This confirmed that it is necessary for MSC to express E1A to produce optimal adenovirus for infection.

We repeated these experiments using EIA+ MSC infected with Ad.iC9-ΔCD19. We assessed ΔCD19 expression in the target cells as a measure of transduction efficiency and iC9 expression. As before, E1A+ MSC produced significantly higher viral titers than E1A− MSC (**Fig. 3c**). Thus MSC can be modified to produce iC9 adenovirus that infects target tumor cells.

Proteasome inhibition sensitizes NSCLC cells to MSC-derived iC9-induced apoptosis and suppresses tumor growth

To determine if tumor cells infected with MSC-derived iC9 can be targeted to undergo apoptosis, we treated infected H1299 cells with CID. Addition of CID significantly increased apoptosis of ΔCD19-positive cells (74% ± 0.98) compared to untreated H1299 cells (**Fig. 3d**). Similar experiments using A549 cells as the target cells showed that CID induced less apoptosis of ΔCD19-positive cells (43.59% ± 6.34) compared to H1299 cells (**Fig. 3e**). This variability in sensitivity to iC9-induced apoptosis was consistent with the differences we observed when we transduced these cell lines directly with iC9. In addition, while bortezomib had little effect on A549 cells infected with iC9, the combination of CID and bortezomib significantly increased apoptosis (81.84±2.55%) compared to untreated cells

(p=<0.0001) or compared to CID treatment (p=0.0006) (**Fig. 3e**). These results confirm that the synergistic effects of bortezomib and CID are maintained when iC9 is delivered by a cellular vehicle.

We next evaluated the *in vivo* consequences of MSC delivery of Ad.iC9 to lung tumor. We used the SCID-Beige mouse lung cancer xenograft model and infused the mice with 2.5×10^6 FFLuc (firefly luciferase) labeled A549 cells intravenously. Following infusion, the cells established tumors in the lung (**Fig. 4a**). Four days following establishment of the tumor, the mice were injected with vehicle or 1×10^6 intravenous AdiC9-E1A-MSC (Day 0 on graph shown in **Fig. 4b**). Two days later, mice were treated with intraperitoneal CID alone (2 to 3 doses every other day), bortezomib alone (twice a week) or a combination of both. This treatment cycle was repeated once for a total of 2 weeks of treatment. As shown in **Fig. 4a-b**, the tumor bioluminescence of mice rapidly increased when the mice were treated with bortezomib alone or infused with AdiC9-E1A-MSC followed by bortezomib treatment (signal change of 1.28E+10 and 1.16E+10 respectively from Day 0 to Day 17). Infusion of AdiC9-E1A-MSC followed by CID treatment diminished tumor growth, (7.03E +9 signal reduction). This effect was further enhanced when AdiC9-E1A-MSC-infused mice were treated with a combination of CID and bortezomib. The combination of CID and bortezomib was significantly more effective than either drug alone (**Fig. 4c**). The attenuation of tumor growth was evident at day 15 following MSC infusion and most significant at day 17 (signal reduction of 2.13E+9) (p=0.002). None of the treatments had any effect on the overall survival of the mice (data not shown). This may be due to severe weight loss observed following bortezomib treatment, which is a known and species idiosyncratic toxicity of bortezomib in mice.[29] These results show that the combination of bortezomib and MSC-delivered inducible caspase-9 attenuates tumor growth in a lung tumor xenograft model.

Active caspase-3 is stabilized by proteasome inhibition.

We next determined the mechanism of bortezomib sensitization to iC9 *in vitro* and *in vivo*. Proteasome inhibition sensitizes cells to apoptosis by preventing degradation of the active forms of caspases including the effector caspase, caspase-3.[30] We first confirmed that cell death in response to the combination of CID and bortezomib was caspase-dependent. We treated iC9-transduced A549 cells with CID and bortezomib as before, in the presence or absence of the caspase inhibitor qVD-OPh. As expected, caspase inhibition completely blocked apoptosis induced by CID, bortezomib and the combination of both drugs (**Fig. 5a**). Since qVD-OPh blocks all caspases, this result strongly indicated that caspase activity was required for the death.

To further explore the effects of CID and bortezomib on caspase activation, we analyzed caspase-9 and caspase-3 cleavage in iC9-transduced H1299 and A549 cells. Following CID treatment of iC9-transduced H1299 cells, iC9 was completely converted from the 45-kD proenzyme to the p17 mature subunit, indicating complete cleavage of the caspase. This effect was accompanied by a corresponding processing of caspase-3 from the 37kD proenzyme to the p20/p17 mature active form, indicating robust caspase activation in response to CID (**Fig. 5b**). Treatment with bortezomib alone resulted in partial cleavage of

caspase-9 as indicated by the intermediate p37 cleavage product in addition to the mature p17 subunit. This was consistent with the ability of bortezomib to induce apoptosis in the absence of CID in these cells.

In iC9-transduced A549 cells, addition of CID induced processing of caspase-9 as full length iC9 was no longer detected by immunoblot. However, we failed to detect any cleaved caspase-9 (p17). Caspase-9-induced cleavage of caspase-3 was also impaired because the proenzyme remained and only very low levels of cleaved caspase-3 were detected (**Fig. 5b**). This suggested that the cleaved forms of these caspases were subject to proteasome-mediated degradation in A549 cells. Consistent with this proposed mechanism, the combination of CID and bortezomib substantially increased the levels of these cleaved products. Hence, the lower levels of cleaved caspase-3 in the lysates of iC9-transduced A549 cells corresponds to the less efficient apoptosis induced by CID observed in this cell line. Together, these data strongly suggest that bortezomib sensitizes iC9-transduced cells to CID by preventing proteasomal degradation of active caspases, thus increasing caspase activity and thereby increasing apoptosis.

Loss of XIAP sensitizes cells to iC9-induced apoptosis

Proteasomal degradation of active caspases is mediated by the inhibitor of apoptosis XIAP,[30] and high levels of XIAP can increase resistance to certain pro-apoptotic stimuli.[31, 32] We measured levels of XIAP protein by immunoblot in the panel of iC9-transduced cell lines to determine if the observed variability in susceptibility to CID-induced apoptosis was associated with differential expression levels of XIAP (**Fig. 5c**). The initial levels of XIAP were comparable in H1299, H441 and A549 cells and were slightly lower in H1650 cells. Transduction of iC9 led to a slight decrease in XIAP protein in all cell lines except for A549 cells. Thus the lower sensitivity of H1650 and A549 cells cannot be explained solely by higher expression levels of XIAP. Exposure to CID resulted in a decrease in XIAP protein in iC9-transduced H1299, H441 and H1650 cells, but not in iC9-transduced A549 cells. Thus in A549 cells, where bortezomib had the greatest effect, XIAP protein persists when caspase-9 is activated.

To further explore the role of XIAP in determining sensitivity to iC9-induced apoptosis, we used shRNA to knockdown XIAP in iC9-transduced A549 cells. We used three different shRNA sequences that targeted XIAP and one resulted in complete stable knockdown (XIAP shRNA#3). (**Fig. 5d**). Under these conditions, treatment of XIAP-knockdown cells with CID resulted in increased apoptosis compared to control knockdown cells (**Fig. 5e**). Knockdown of XIAP also sensitized iC9-A549 cells to apoptosis induced by bortezomib. This mirrors the effect of bortezomib in iC9-transduced H1299 cells shown in Figure 2. Together these findings suggest that the inhibitory activity of XIAP contributes to the degradation of active caspase-3, which is overcome by inhibition of the proteasome resulting in a corresponding increase in the potency of CID-dependent, iC9-mediated apoptosis.

DISCUSSION

While adenoviral vectors have been extensively used for cancer therapies, only modest benefits have been observed.[33-35] One of the limitations to success has been rapid clearance

of the vector by the host's innate and adaptive immune systems, with consequent limited biodistribution to tumor sites.[19] Investigators have therefore developed “stealth” vectors that are sheltered from the immune system within cells and whose delivery depends on the biodistribution of the sheltering cell and not of the vector itself. We now describe how this concept can be applied to NSCLC by taking advantage of the selective accumulation of MSC in the lung vasculature at sites of tumor.[21, 24, 36] We have engineered these MSC to produce an adenoviral vector encoding the *inducible caspase 9* (*iC9*) gene (**Fig. 6**). We have shown that this approach can be used to kill NSCLC *in vitro* and in an orthotopic mouse xenograft model of lung cancer. Furthermore, the effects are synergistically enhanced by combining the MSC-Ad.iC9 with administration of the proteasome inhibitor bortezomib, a drug that is otherwise ineffective for the treatment of NSCLC.

MSC have characteristics that make them well suited as cellular vehicles for delivery of anti-tumor agents such as AdV-iC9 to lung tumors. They can be reliably isolated from bone marrow and expanded to large numbers *in vitro*.[37] In addition, they lack MHC II and co-stimulatory molecule expression, allowing them to be used in an allogeneic setting with minimal immunogenicity.[38] These properties have encouraged the use of MSC for targeted delivery of a diverse array of anti-tumor agents to tumor sites. MSC have successfully delivered tumor necrosis factor apoptosis-inducing ligand (TRAIL), Interleukin-12, interferon, suicide genes or a combination of potentially oncolytic agents to an array of tumors including gliomas, cervical carcinoma, pancreatic cancer, colon cancer, melanoma and renal cell carcinoma.[14-17] MSC become entrapped in the lung microvasculature after intravenous administration,[21] and migrate toward “inflammatory” sites including tumors.[23] The current study exploits these properties of MSC to deliver the iC9 suicide gene to NSCLC cells.

Most studies that deliver suicide genes to cancer cells have used strategies involving nucleoside analogs, such as those combining Herpes Simplex Virus thymidine kinase (HSV-TK) with ganciclovir (GCV)[39] and bacterial or yeast cytosine deaminase (CD) with 5-fluoro-cytosine (5-FC)[40, 41] to induce cell death. These systems have the advantages of producing significant bystander killing due to transfer or release of the phosphorylated nucleosides formed from the nucleoside pro-drugs.[42] Nonetheless, the potential benefits of these systems are limited by a number of inherent deficiencies. Both HSV-TK/GCV and CD/5-FC kill cells by interfering with DNA synthesis, so that the approach has its greatest effects on tumor cells that are in cell cycle. This leaves significant residual cell populations in slower growing regions of the tumor, and may have limited impact on the slowly dividing stromal elements that are critical for tumor cell growth and treatment resistance. Even for cycling cells, the effects may be slow in onset favoring the emergence of resistant cells.[43] Although immune response has been shown to increase the efficacy of the HSV-TK/GCV system in liver tumors,[44] the immunogenicity of the transgene product may alternately cause transduced cells to be eliminated by the immune system before sufficient phosphonucleosides are produced for a significant bystander effect on adjacent tumor cells.[45] Finally, the pro-drugs required may be toxic (e.g. 5-FC) particularly in heavily pretreated cancer patients, or may have additional therapeutic uses that would be excluded (e.g., GCV).[46]

For these reasons, delivery of the *iC9* suicide gene in combination with CID represents a valuable complement to existing methods for inducing cancer cell death. A study in human recipients of stem cell transplantation showed that a single dose of CID efficiently and rapidly induced apoptosis of T cells expressing iC9.[3] Since iC9 works by directly inducing apoptosis, this rapid activity occurs irrespective of the cell cycle status of the transgenic cells unlike HSV-TK. Moreover, the *iC9* transgene encodes a protein that is almost entirely derived of human sequences, and appears to lack immunogenicity. Importantly, CID is a bioinert small molecule that has shown no evidence of toxicities even at doses 10-fold higher than those required to activate iC9.[3, 28]

The iC9-CID system takes advantage of the fact that caspase-9 is activated by dimerization.[6] Enforced dimerization of caspase-9 is mediated by the FKBP dimerization domain that is fused to caspase-9, resulting in rapid activation of downstream caspases, including the effector caspase, caspase-3, and apoptosis. In normal cells, caspase-9 is activated by cytochrome c, following its release from mitochondria. Many cytotoxic drugs induce apoptosis by engaging this pathway and inducing cytochrome c release.[47] iC9 is engaged downstream of this step and hence is a more direct way of inducing apoptosis in the absence of any additional upstream signals. Theoretically, this mode of inducing apoptosis should be less prone to inhibition than traditional chemotherapeutic regimens that engage the mitochondrial pathway. For example, drug resistance in cancer cells is often associated with increased expression of the anti-apoptotic protein Bcl-2, which blocks cytochrome c release from the mitochondria.[8] Direct activation of caspase-9 independent of this step should overcome such resistance mechanisms.

Despite the potential advantages of this system our results demonstrate that lung cancer cells exhibit substantial heterogeneity in their sensitivity to iC9-induced cell death. The relative resistance we observed in certain NSCLC cells was effectively overcome by combining iC9 and the proteasome inhibitor bortezomib. Bortezomib is a boronic-acid derivative that reversibly inhibits the active sites in the 20S proteasome. It has shown excellent clinical activity in patients with multiple myeloma[48] but its single agent activity in solid tumors has been less impressive.[49, 50] The mechanism of action of bortezomib is not fully understood but it appears to have broad effects on cancer cells including down-regulating the pro-oncogenic NFκB pathway,[51, 52] stabilizing pro-apoptotic proteins,[53] increasing protein toxicity and enhancing autophagy.[54]

The combination of CID and bortezomib enhanced the anti-tumor activity of MSC delivered iC9 in a xenograft model of lung cancer. However, the combination of CID and bortezomib did not prolong survival of the mice. This appeared to be due to species-dependent non-specific toxic effects of bortezomib, including severe weight loss. Similar effects have been previously reported in mice following multi-dose treatment with bortezomib as a single agent.[29] Although bortezomib is known to induce transient thrombocytopenia when given at therapeutic doses in humans, the more severe toxic side-effects seen in mice are not replicated.[29] Therefore it should be feasible to test the combination of iC9 and bortezomib clinically, should additional pre-clinical studies confirm their synergistic activity. Our translational path currently envisages the use of a conditionally replication competent adenovirus[55] encoding iC9, thereby providing both an amplification step for iC9 expression

and an additional mechanism for tumor destruction. Our proposed phase I study will use MSC delivery of iC9 alone, followed by a second cohort of patients who will be treated with the combination of iC9 and bortezomib at approved doses.

The potential for toxicity also underscores the need to understand the mechanism by which bortezomib enhances apoptosis and tumor killing induced by caspase-9 in order to identify further ways to improve this therapeutic strategy. Bortezomib appears to function in this context by preventing proteasomal-mediated degradation of pro-apoptotic mature caspases. We observed enhanced stabilization of the processed forms of both caspase-9 and caspase-3 in response to combined CID and bortezomib treatment. Our data further suggest that this stabilization is mediated through effects on XIAP, a member of the inhibitor of apoptosis protein (IAP) family and a potent inhibitor of caspase-3, -7 and -9.[56] XIAP is an E3 ubiquitin ligase that binds caspase-3 and targets it to the proteasome for degradation.[30, 57] Knockdown of XIAP sensitized cells to iC9-induced apoptosis, suggesting that bortezomib maximizes iC9-induced apoptosis, in part, by antagonizing the E3 ligase activity of XIAP (**Fig. 6**). Bortezomib also down-regulates NFκB signaling.[51] XIAP is a transcriptional target of NFκB,[58] therefore bortezomib may further down-regulate XIAP activity by reducing its expression level.

Upregulation of IAPs or their aberrant expression by tumor cells has been associated with therapy resistance and poor prognosis.[59-62] Strategies targeting IAPs using small molecule IAP-antagonists represent a promising approach to overcome drug-resistance.[63] For example, inhibition of XIAP has been shown to potentiate TRAIL induced apoptosis and overcome resistance to TRAIL in a number of pre-clinical cancer models.[64-67] Similarly, the requirement to overcome XIAP activity for maximal induction of iC9-associated apoptosis may also suggest a clinical application for the use of IAP-antagonists in combination with MSC-delivered iC9.

Unlike HSV-TK/GCV, the mode of action of iC9/CID does not allow for bystander killing of uninfected cells by transgene products from the transduced tumor cells. Having validated the concept of delivering iC9 in an adenoviral vector by means of MSC it should now be possible to further develop the approach so that the effect of iC9 can be amplified. For example, as described above, a conditionally replicating iC9 adenoviral vector could be substituted for the replication incompetent vector used in these initial validation studies.[68] The current iC9 vector could also be modified to incorporate one or more immunostimulatory genes to allow the cells killed by iC9/CID to generate a more generalized anti-tumor immune response.[69] Both approaches could be extended to this novel MSC-iC9 system.

In conclusion, this study is the first to demonstrate the feasibility and potential effectiveness of systemic administration of Ad-iC9 producing MSC for NSCLC treatment. The anti-tumor activity is synergistically enhanced when the approach is combined with the proteasomal inhibitor bortezomib, a drug that is otherwise inactive against NSCLC.[50]

Supplementary Material

Refer to Web version on PubMed Central for supplementary material.

Acknowledgments

This work was supported by the Cancer Prevention Research Institute of Texas RP110553 P1 (MKB) and the National Institutes of Health T32 HL092332 and T32DK060445 (VH).

References

1. Duarte S, Carle G, Faneca H, de Lima MC, Pierrefite-Carle V. Suicide gene therapy in cancer: where do we stand now? Cancer Lett. 2012; 324(2):160–170. [PubMed: 22634584]
2. Mohit E, Rafati S. Biological delivery approaches for gene therapy: Strategies to potentiate efficacy and enhance specificity. Mol Immunol. 2013; 56(4):599–611. [PubMed: 23911418]
3. Di Stasi A, Tey SK, Dotti G, Fujita Y, Kennedy-Nasser A, Martinez C, et al. Inducible apoptosis as a safety switch for adoptive cell therapy. N Engl J Med. 2011; 365(18):1673–1683. [PubMed: 22047558]
4. Ramos CA, Asgari Z, Liu E, Yvon E, Heslop HE, Rooney CM, et al. An inducible caspase 9 suicide gene to improve the safety of mesenchymal stromal cell therapies. Stem Cells. 2010; 28(6):1107–1115. [PubMed: 20506146]
5. Straathof KC, Pule MA, Yotnda P, Dotti G, Vanin EF, Brenner MK, et al. An inducible caspase 9 safety switch for T-cell therapy. Blood. 2005; 105(11):4247–4254. [PubMed: 15728125]
6. Boatright KM, Renatus M, Scott FL, Sperandio S, Shin H, Pedersen IM, et al. A unified model for apical caspase activation. Mol Cell. 2003; 11(2):529–541. [PubMed: 12620239]
7. Riedl SJ, Salvesen GS. The apoptosome: signalling platform of cell death. Nat Rev Mol Cell Biol. 2007; 8(5):405–413. [PubMed: 17377525]
8. Yang J, Liu X, Bhalla K, Kim CN, Ibrado AM, Cai J, et al. Prevention of apoptosis by Bcl-2: release of cytochrome c from mitochondria blocked. Science. 1997; 275(5303):1129–1132. [PubMed: 9027314]
9. Naumann I, Kappler R, von Schweinitz D, Debatin KM, Fulda S. Bortezomib primes neuroblastoma cells for TRAIL-induced apoptosis by linking the death receptor to the mitochondrial pathway. Clin Cancer Res. 2011; 17(10):3204–3218. [PubMed: 21459798]
10. Yang HH, Ma MH, Vescio RA, Berenson JR. Overcoming drug resistance in multiple myeloma: the emergence of therapeutic approaches to induce apoptosis. J Clin Oncol. 2003; 21(22):4239–4247. [PubMed: 14615454]
11. Miller CP, Ban K, Dujka ME, McConkey DJ, Munsell M, Palladino M, et al. NPI-0052, a novel proteasome inhibitor, induces caspase-8 and ROS-dependent apoptosis alone and in combination with HDAC inhibitors in leukemia cells. Blood. 2007; 110(1):267–277. [PubMed: 17356134]
12. Goel A, Dispenzieri A, Greipp PR, Witzig TE, Mesa RA, Russell SJ. PS-341-mediated selective targeting of multiple myeloma cells by synergistic increase in ionizing radiation-induced apoptosis. Exp Hematol. 2005; 33(7):784–795. [PubMed: 15963854]
13. McConkey DJ, Zhu K. Mechanisms of proteasome inhibitor action and resistance in cancer. Drug Resist Updat. 2008; 11(4-5):164–179. [PubMed: 18818117]
14. Gao P, Ding Q, Wu Z, Jiang H, Fang Z. Therapeutic potential of human mesenchymal stem cells producing IL-12 in a mouse xenograft model of renal cell carcinoma. Cancer Lett. 2010; 290(2):157–166. [PubMed: 19786319]
15. Grisendi G, Bussolari R, Cafarelli L, Petak I, Rasini V, Veronesi E, et al. Adipose-derived mesenchymal stem cells as stable source of tumor necrosis factor-related apoptosis-inducing ligand delivery for cancer therapy. Cancer Res. 2010; 70(9):3718–3729. [PubMed: 20388793]
16. Matuskova M, Hlubinova K, Pastorakova A, Hunakova L, Altanerova V, Altaner C, et al. HSV-tk expressing mesenchymal stem cells exert bystander effect on human glioblastoma cells. Cancer Lett. 2010; 290(1):58–67. [PubMed: 19765892]

17. Studeny M, Marini FC, Champlin RE, Zompetta C, Fidler IJ, Andreeff M. Bone marrow-derived mesenchymal stem cells as vehicles for interferon-beta delivery into tumors. Cancer Res. 2002; 62(13):3603–3608. [PubMed: 12097260]
18. Wang Y, Hu JK, Krol A, Li YP, Li CY, Yuan F. Systemic dissemination of viral vectors during intratumoral injection. Mol Cancer Ther. 2003; 2(11):1233–1242. [PubMed: 14617797]
19. Worgall S, Wolff G, Falck-Pedersen E, Crystal RG. Innate immune mechanisms dominate elimination of adenoviral vectors following in vivo administration. Hum Gene Ther. 1997; 8(1): 37–44. [PubMed: 8989993]
20. Dembinski JL, Spaeth EL, Fueyo J, Gomez-Manzano C, Studeny M, Andreeff M, et al. Reduction of nontarget infection and systemic toxicity by targeted delivery of conditionally replicating viruses transported in mesenchymal stem cells. Cancer Gene Ther. 2010; 17(4):289–297. [PubMed: 19876078]
21. Fischer UM, Harting MT, Jimenez F, Monzon-Posadas WO, Xue H, Savitz SI, et al. Pulmonary passage is a major obstacle for intravenous stem cell delivery: the pulmonary first-pass effect. Stem Cells Dev. 2009; 18(5):683–692. [PubMed: 19099374]
22. Loebinger MR, Janes SM. Stem cells as vectors for antitumour therapy. Thorax. 2010; 65(4):362–369. [PubMed: 20388765]
23. Fritz V, Jorgensen C. Mesenchymal stem cells: an emerging tool for cancer targeting and therapy. Curr Stem Cell Res Ther. 2008; 3(1):32–42. [PubMed: 18220921]
24. Loebinger MR, Kyrtatos PG, Turmaine M, Price AN, Pankhurst Q, Lythgoe MF, et al. Magnetic resonance imaging of mesenchymal stem cells homing to pulmonary metastases using biocompatible magnetic nanoparticles. Cancer Res. 2009; 69(23):8862–8867. [PubMed: 19920196]
25. Tey SK, Dotti G, Rooney CM, Heslop HE, Brenner MK. Inducible caspase 9 suicide gene to improve the safety of allodepleted T cells after haploidentical stem cell transplantation. Biol Blood Marrow Transplant. 2007; 13(8):913–924. [PubMed: 17640595]
26. Vera J, Savoldo B, Vigouroux S, Biagi E, Pule M, Rossig C, et al. T lymphocytes redirected against the kappa light chain of human immunoglobulin efficiently kill mature B lymphocyte-derived malignant cells. Blood. 2006; 108(12):3890–3897. [PubMed: 16926291]
27. Zhou LJ, Ord DC, Hughes AL, Tedder TF. Structure and domain organization of the CD19 antigen of human, mouse, and guinea pig B lymphocytes. Conservation of the extensive cytoplasmic domain. J Immunol. 1991; 147(4):1424–1432. [PubMed: 1714482]
28. Iuliucci JD, Oliver SD, Morley S, Ward C, Ward J, Dalgarno D, et al. Intravenous safety and pharmacokinetics of a novel dimerizer drug, AP1903, in healthy volunteers. J Clin Pharmacol. 2001; 41(8):870–879. [PubMed: 11504275]
29. Lonial S, Waller EK, Richardson PG, Jagannath S, Orlowski RZ, Giver CR, et al. Risk factors and kinetics of thrombocytopenia associated with bortezomib for relapsed, refractory multiple myeloma. Blood. 2005; 106(12):3777–3784. [PubMed: 16099887]
30. Suzuki Y, Nakabayashi Y, Takahashi R. Ubiquitin-protein ligase activity of X-linked inhibitor of apoptosis protein promotes proteasomal degradation of caspase-3 and enhances its anti-apoptotic effect in Fas-induced cell death. Proc Natl Acad Sci U S A. 2001; 98(15):8662–8667. [PubMed: 11447297]
31. Albeck JG, Burke JM, Aldridge BB, Zhang M, Lauffenburger DA, Sorger PK. Quantitative analysis of pathways controlling extrinsic apoptosis in single cells. Mol Cell. 2008; 30(1):11–25. [PubMed: 18406323]
32. Rehm M, Huber HJ, Dussmann H, Prehn JH. Systems analysis of effector caspase activation and its control by X-linked inhibitor of apoptosis protein. EMBO J. 2006; 25(18):4338–4349. [PubMed: 16932741]
33. Sterman DH, Treat J, Litzky LA, Amin KM, Coonrod L, Molnar-Kimber K, et al. Adenovirus-mediated herpes simplex virus thymidine kinase/ganciclovir gene therapy in patients with localized malignancy: results of a phase I clinical trial in malignant mesothelioma. Hum Gene Ther. 1998; 9(7):1083–1092. [PubMed: 9607419]
34. Xu F, Li S, Li XL, Guo Y, Zou BY, Xu R, et al. Phase I and biodistribution study of recombinant adenovirus vector-mediated herpes simplex virus thymidine kinase gene and ganciclovir

administration in patients with head and neck cancer and other malignant tumors. Cancer Gene Ther. 2009; 16(9):723–730. [PubMed: 19363470]

35. Alvarez RD, Gomez-Navarro J, Wang M, Barnes MN, Strong TV, Arani RB, et al. Adenoviral-mediated suicide gene therapy for ovarian cancer. Mol Ther. 2000; 2(5):524–530. [PubMed: 11082326]
36. Gholamrezanezhad A, Mirpour S, Bagheri M, Mohamadnejad M, Alimoghaddam K, Abdolahzadeh L, et al. In vivo tracking of 111In-oxine labeled mesenchymal stem cells following infusion in patients with advanced cirrhosis. Nucl Med Biol. 2011; 38(7):961–967. [PubMed: 21810549]
37. Zhou DH, Huang SL, Wu YF, Wei J, Chen GY, Li Y, et al. [The expansion and biological characteristics of human mesenchymal stem cells]. Zhonghua Er Ke Za Zhi. 2003; 41(8):607–610. [PubMed: 14744385]
38. Koppula PR, Chelluri LK, Polisetti N, Vemuganti GK. Histocompatibility testing of cultivated human bone marrow stromal cells - a promising step towards pre-clinical screening for allogeneic stem cell therapy. Cell Immunol. 2009; 259(1):61–65. [PubMed: 19577229]
39. Moolten FL. Tumor chemosensitivity conferred by inserted herpes thymidine kinase genes: paradigm for a prospective cancer control strategy. Cancer Res. 1986; 46(10):5276–5281. [PubMed: 3019523]
40. Kievit E, Bershad E, Ng E, Sethna P, Dev I, Lawrence TS, et al. Superiority of yeast over bacterial cytosine deaminase for enzyme/prodrug gene therapy in colon cancer xenografts. Cancer Res. 1999; 59(7):1417–1421. [PubMed: 10197605]
41. Mullen CA, Kilstrup M, Blaese RM. Transfer of the bacterial gene for cytosine deaminase to mammalian cells confers lethal sensitivity to 5-fluorocytosine: a negative selection system. Proc Natl Acad Sci U S A. 1992; 89(1):33–37. [PubMed: 1729703]
42. Freeman SM, Abboud CN, Whartenby KA, Packman CH, Koeplin DS, Moolten FL, et al. The “bystander effect”: tumor regression when a fraction of the tumor mass is genetically modified. Cancer Res. 1993; 53(21):5274–5283. [PubMed: 8221662]
43. Zhang L, Wikenheiser KA, Whitsett JA. Limitations of retrovirus-mediated HSV-tk gene transfer to pulmonary adenocarcinoma cells in vitro and in vivo. Hum Gene Ther. 1997; 8(5):563–574. [PubMed: 9095408]
44. Agard C, Ligeza C, Dupas B, Izembart A, El Kouri C, Moullier P, et al. Immune-dependent distant bystander effect after adenovirus-mediated suicide gene transfer in a rat model of liver colorectal metastasis. Cancer Gene Ther. 2001; 8(2):128–136. [PubMed: 11263528]
45. Traversari C, Marktel S, Magnani Z, Mangia P, Russo V, Ciceri F, et al. The potential immunogenicity of the TK suicide gene does not prevent full clinical benefit associated with the use of TK-transduced donor lymphocytes in HSCT for hematologic malignancies. Blood. 2007; 109(11):4708–4715. [PubMed: 17327417]
46. Jacobsen T, Sifontis N. Drug interactions and toxicities associated with the antiviral management of cytomegalovirus infection. Am J Health Syst Pharm. 2010; 67(17):1417–1425. [PubMed: 20720240]
47. Kaufmann SH, Earnshaw WC. Induction of apoptosis by cancer chemotherapy. Exp Cell Res. 2000; 256(1):42–49. [PubMed: 10739650]
48. Richardson PG, Sonneveld P, Schuster M, Irwin D, Stadtmauer E, Facon T, et al. Extended follow-up of a phase 3 trial in relapsed multiple myeloma: final time-to-event results of the APEX trial. Blood. 2007; 110(10):3557–3560. [PubMed: 17690257]
49. Aghajanian C, Blessing JA, Darcy KM, Reid G, DeGeest K, Rubin SC, et al. A phase II evaluation of bortezomib in the treatment of recurrent platinum-sensitive ovarian or primary peritoneal cancer: a Gynecologic Oncology Group study. Gynecol Oncol. 2009; 115(2):215–220. [PubMed: 19712963]
50. Hoang T, Campbell TC, Zhang C, Kim K, Kolesar JM, Oettel KR, et al. Vorinostat and bortezomib as third-line therapy in patients with advanced non-small cell lung cancer: a Wisconsin Oncology Network Phase II study. Invest New Drugs. 2013; 32(1):195–199. [PubMed: 23728919]

51. Hideshima T, Ikeda H, Chauhan D, Okawa Y, Raje N, Podar K, et al. Bortezomib induces canonical nuclear factor-kappaB activation in multiple myeloma cells. Blood. 2009; 114(5):1046–1052. [PubMed: 19436050]
52. Bu R, Hussain AR, Al-Obaisi KA, Ahmed M, Uddin S, Al-Kuraya KS. Bortezomib inhibits proteasomal degradation of IkappaBalpha and induces mitochondrial dependent apoptosis in activated B-cell diffuse large B-cell lymphoma. Leuk Lymphoma. 2013; 55(2):415–424. [PubMed: 23697845]
53. Foti C, Florean C, Pezzutto A, Roncaglia P, Tomasella A, Gustincich S, et al. Characterization of caspase-dependent and caspase-independent deaths in glioblastoma cells treated with inhibitors of the ubiquitin-proteasome system. Mol Cancer Ther. 2009; 8(11):3140–3150. [PubMed: 19887551]
54. Ding WX, Ni HM, Gao W, Yoshimori T, Stolz DB, Ron D, et al. Linking of autophagy to ubiquitin-proteasome system is important for the regulation of endoplasmic reticulum stress and cell viability. Am J Pathol. 2007; 171(2):513–524. [PubMed: 17620365]
55. Alonso MM, Gomez-Manzano C, Jiang H, Bekele NB, Piao Y, Yung WK, et al. Combination of the oncolytic adenovirus ICOVIR-5 with chemotherapy provides enhanced anti-glioma effect in vivo. Cancer Gene Ther. 2007; 14(8):756–761. [PubMed: 17557108]
56. Deveraux QL, Takahashi R, Salvesen GS, Reed JC. X-linked IAP is a direct inhibitor of cell-death proteases. Nature. 1997; 388(6639):300–304. [PubMed: 9230442]
57. Chen L, Smith L, Wang Z, Smith JB. Preservation of caspase-3 subunits from degradation contributes to apoptosis evoked by lactacystin: any single lysine or lysine pair of the small subunit is sufficient for ubiquitination. Mol Pharmacol. 2003; 64(2):334–345. [PubMed: 12869638]
58. Stehlik C, de Martin R, Kumabashiri I, Schmid JA, Binder BR, Lipp J. Nuclear factor (NF)-kappaB-regulated X-chromosome-linked iap gene expression protects endothelial cells from tumor necrosis factor alpha-induced apoptosis. J Exp Med. 1998; 188(1):211–216. [PubMed: 9653098]
59. Yang XH, Feng ZE, Yan M, Hanada S, Zuo H, Yang CZ, et al. XIAP is a predictor of cisplatin-based chemotherapy response and prognosis for patients with advanced head and neck cancer. PLoS One. 2012; 7(3):e31601. [PubMed: 22403616]
60. Moussata D, Amara S, Siddeek B, Decaussin M, Hehlgans S, Paul-Bellon R, et al. XIAP as a radioresistance factor and prognostic marker for radiotherapy in human rectal adenocarcinoma. Am J Pathol. 2012; 181(4):1271–1278. [PubMed: 22867709]
61. Zhang Y, Zhu J, Tang Y, Li F, Zhou H, Peng B, et al. X-linked inhibitor of apoptosis positive nuclear labeling: a new independent prognostic biomarker of breast invasive ductal carcinoma. Diagn Pathol. 2011; 6:49. [PubMed: 21645409]
62. Ibrahim AM, Mansour IM, Wilson MM, Mokhtar DA, Helal AM, Al Wakeel HM. Study of survivin and X-linked inhibitor of apoptosis protein (XIAP) genes in acute myeloid leukemia (AML). Lab Hematol. 2012; 18(1):1–10. [PubMed: 22459568]
63. Chen DJ, Huerta S. Smac mimetics as new cancer therapeutics. Anticancer Drugs. 2009; 20(8): 646–658. [PubMed: 19550293]
64. Wu MS, Wang GF, Zhao ZQ, Liang Y, Wang HB, Wu MY, et al. Smac Mimetics in Combination with TRAIL Selectively Target Cancer Stem Cells in Nasopharyngeal Carcinoma. Mol Cancer Ther. 2013; 12(9):1728–1737. [PubMed: 23699656]
65. Allensworth JL, Sauer SJ, Lyerly HK, Morse MA, Devi GR. Smac mimetic Birinapant induces apoptosis and enhances TRAIL potency in inflammatory breast cancer cells in an IAP-dependent and TNF-alpha-independent mechanism. Breast Cancer Res Treat. 2013; 137(2):359–371. [PubMed: 23225169]
66. Dai Y, Liu M, Tang W, Li Y, Lian J, Lawrence TS, et al. A Smac-mimetic sensitizes prostate cancer cells to TRAIL-induced apoptosis via modulating both IAPs and NF-kappaB. BMC Cancer. 2009; 9:392. [PubMed: 19895686]
67. Bockbrader KM, Tan M, Sun Y. A small molecule Smac-mimic compound induces apoptosis and sensitizes TRAIL-and etoposide-induced apoptosis in breast cancer cells. Oncogene. 2005; 24(49): 7381–7388. [PubMed: 16044155]
68. Yong RL, Shinojima N, Fueyo J, Gumin J, Vecil GG, Marini FC, et al. Human bone marrow-derived mesenchymal stem cells for intravascular delivery of oncolytic adenovirus Delta24-RGD to human gliomas. Cancer Res. 2009; 69(23):8932–8940. [PubMed: 19920199]

69. Colombo F, Barzon L, Franchin E, Pacenti M, Pinna V, Danieli D, et al. Combined HSV TK/IL-2 gene therapy in patients with recurrent glioblastoma multiforme: biological and clinical results. Cancer Gene Ther. 2005; 12(10):835–848. [PubMed: 15891772]

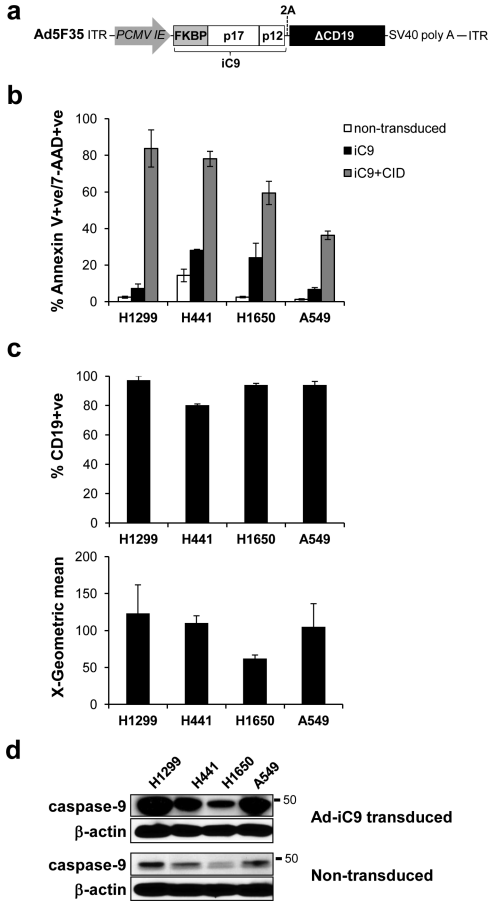

Figure 1.

CID induces iC9-dependent apoptosis in transduced NSCLC cell lines. **(a)** Schematic representation of the adenoviral iC9 bi-cistronic vector. The construct contains the suicide gene iC9 and truncated CD19 (ΔCD19) as a marker separated by a 2A sequence. **(b)** NSCLC cell lines were transduced with Ad-iC9. 48 hr later cells were left untreated or treated with CID (80nM). Apoptosis was assessed by flow cytometry for Annexin V binding and 7-AAD staining 24 hours after treatment. Error bars represent standard deviation. **(c)** iC9-transduced cells were assessed for ΔCD19 expression and corresponding MFI by flow cytometry for staining with anti-CD19 antibody 72 hr following transduction. **(d)** Lysates from cells in (c) and non-transduced cells were blotted for the presence of caspase-9 with an anti-caspase-9 antibody.

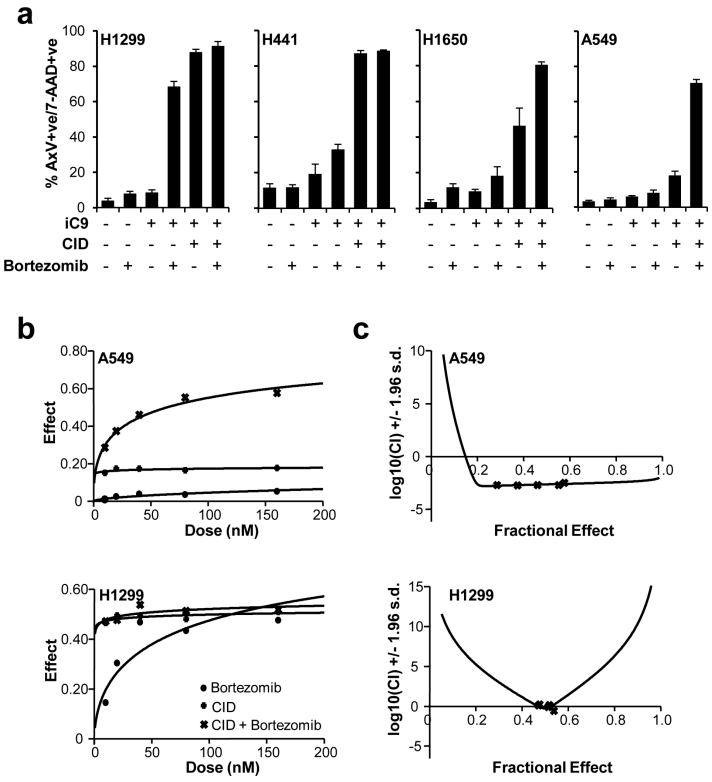

Figure 2.

Bortezomib enhances CID-induced apoptosis of iC9-transduced cells. **(a)** Non transduced and iC9-transduced NSCLC cell lines were left untreated or treated with bortezomib (80 nM) in the presence or absence of CID (80 nM) as indicated. Apoptosis was assessed by flow cytometry for Annexin V binding and 7-AAD staining 24 hours after treatment. Error bars represent standard deviation. **(b)** iC9-transduced A549 and H1299 cells were treated with the indicated amounts of CID, bortezomib or a combination of both. Apoptosis was assessed by flow cytometry for Annexin V binding and 7-AAD staining 24 hours after treatment (see Figure S2). Dose-effect curves were plotted using CalcuSyn™ software. **(c)** Combination indices were calculated from the data in (b) and plotted using CalcuSyn™ software. CI value less than 1.0 is considered synergistic.

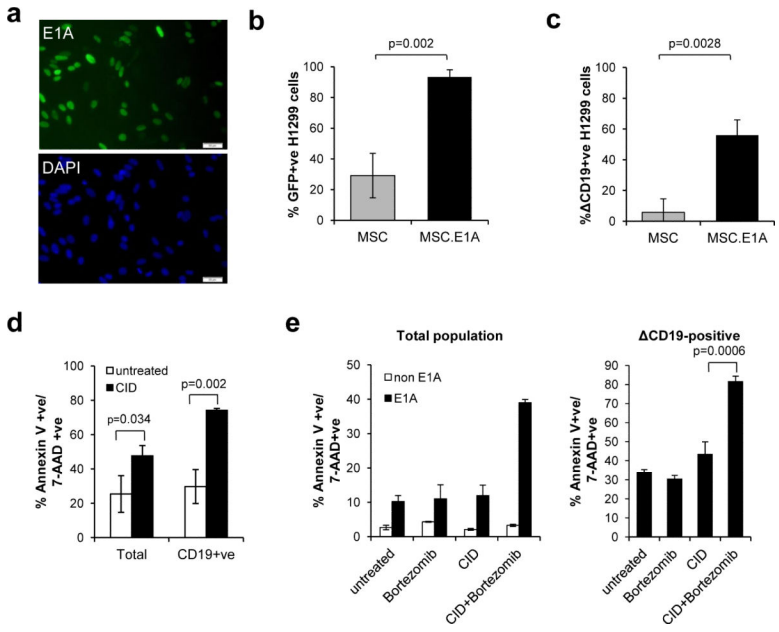

Figure 3.

E1A-modified MSC deliver Ad-iC9 to tumor cells that are targeted to undergo apoptosis with CID and bortezomib. **(a)** MSC were transduced with retrovirus encoding the E1A gene. Five days later cells were fixed and stained with anti-E1A antibody and an Alexa Fluor 488-conjugated secondary antibody (green) and counter-stained with DAPI (blue). Representative images of 1 of 5 donors showing E1A expression in the nuclei of 40-60% of MSC. Scale bars represent 50μm. **(b)** H1299 cells were incubated with supernatant from Ad.GFP-transduced MSC or Ad.GFP-transduced MSC expressing E1A. GFP expression was measured by flow cytometry 3 days later. Error bars represent standard deviation. **(c)** H1299 cells were incubated with supernatant from Ad.iC9-transduced MSC or Ad.iC9-transduced MSC expressing E1A. iC9 expression was assessed by flow cytometry for CD19 staining 3 days later. Error bars represent standard deviation. **(d)** H1299 cells were infected with Ad.iC9 as in (c) followed by treatment with CID (80 nM). Apoptosis was assessed by flow cytometry for Annexin V binding and 7-AAD staining 24 hours after treatment. Error bars represent standard deviation. **(e)** A549 cells were incubated with supernatant from Ad.iC9-transduced MSC or Ad.iC9-transduced MSC expressing E1A for 3 days. Cells were left untreated or treated with CID (80 nM), bortezomib (80 nM), or both. Apoptosis was assessed by flow cytometry for Annexin V binding and 7-AAD staining 24 hours after treatment (*left*). Cells incubated with supernatants from E1A positive MSC were gated for ΔCD19 expression and the results are shown (*right*). Error bars represent standard deviation.

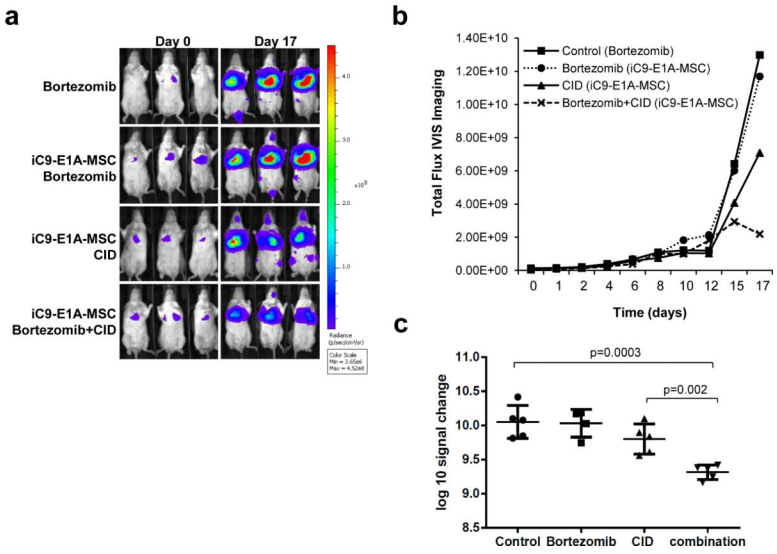

Figure 4.

AdiC9-E1A-MSC treatment in combination with bortezomib suppresses tumor growth. **(a)** SCID-Beige mice were engrafted with FFluc-labeled A549 cells intravenously (IV) followed by IV infusion with iC9-E1A-MSC where indicated. Mice received intraperitoneal injections of CID (50 μg), bortezomib (0.3 mg/kg) or both as described in “Methods”. Tumor growth was monitored by in vivo imaging to measure bioluminescence. Representative images of bioluminescence in mice show the tumor site and tumor size on Day 0 and Day 17. **(b)** Growth of tumors from mice in each treatment group was measured by assessing mean bioluminescence (5 mice per group). **(c)** Total tumor growth after 17 days is represented as log10 signal change. Error bars represent standard deviation.

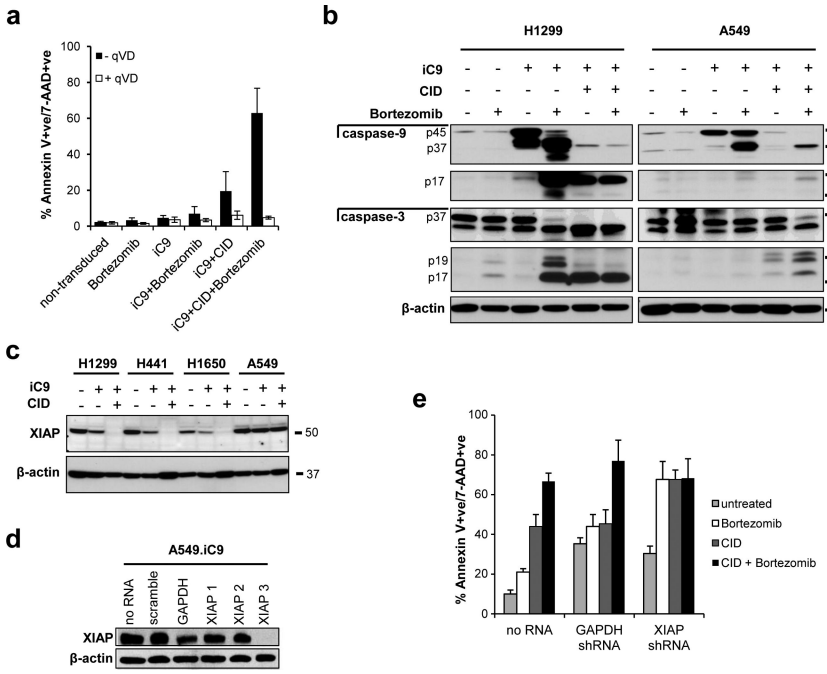

Figure 5.

Proteasome inhibition enhances stabilization of active caspase-3**. (a)** iC9-transduced A549 cells were left untreated or treated with CID (200 nM), bortezomib (80 nM), or a combination of both in the presence or absence of qVD-OPH (20 μM). Apoptosis was assessed by flow cytometry for Annexin V binding and 7-AAD staining 24 hours after treatment. Error bars represent standard deviation. (**b**) Non-transduced or Ad-iC9-transduced H1299 cells (*left*) or non-transduced or Ad-iC9-transduced A549 cells (right) were treated with bortezomib (80 nM), CID (200 nM) or both as indicated, and lysates were made 24 hr later. Equal amounts of total protein were analyzed by immunoblotting for caspase-9, cleaved caspase-9, caspase-3, cleaved caspase-3 or actin (as a loading control). **(c)** NSCLC cell lines or iC9-transduced NSCLC cell lines were left untreated or treated with CID (200 nM) as indicated, and lysates were made 24 hr later. Equal amounts of total protein were analyzed by immunoblotting for XIAP expression or actin (as a loading control). **(d)** A549 cells were stably transduced with non-targeting (scramble) shRNA, control shRNA (GAPDH) or three different shRNAs targeting *XIAP* (XIAP1, XIAP2 and XIAP3). Whole cell lysates were analyzed for XIAP knockdown by immunoblot. (**e**) A549 cells, XIAP knockdown A549 cells (using XIAP3 shRNA) or GAPDH knockdown A549 cells were transduced with Ad.iC9 followed by treatment with bortezomib (80nM), CID (200nM) or both. Apoptosis was assessed by flow cytometry for Annexin V binding and 7-AAD staining 24 hours after treatment. Error bars represent standard deviation.

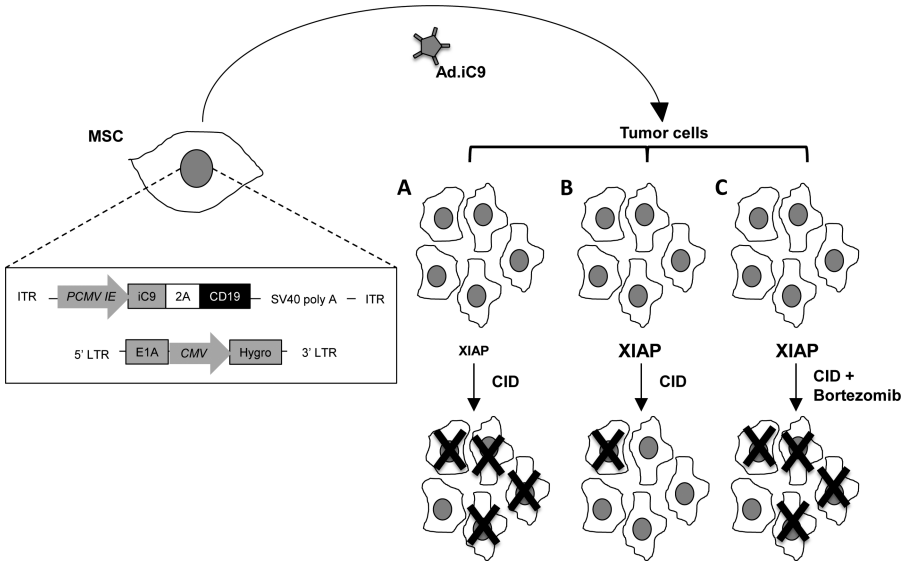

Figure 6.

Proposed model for iC9-E1A-MSC therapy. Schematic representation of MSC modified to express E1A via retroviral transduction and iC9 via adenoviral transduction is shown (*left*). Infused iC9-E1A-MSC migrate toward the tumor site where they release Ad.iC9, which, in turn, infects lung tumor cells. When tumor cells that have low XIAP activity are infected with Ad.iC9 and exposed to CID, the majority of them will undergo apoptosis (**A**). When XIAP activity is high, CID will have little effect as XIAP targets active caspases to the proteasome **(B)**. XIAP activity in the latter tumors can be overcome by further treatment with bortezomib to block proteasome-mediated degradation of active caspases, enhancing apoptosis **(C)**.